The Unique Properties of ω Centauri Seen Through Strömgren Eyes*

M. Hilker [1] and T. Richtler[2]

[1]Departamento de Astronomía y Astrofísica, P. Universidad Católica, Chile
[2]Departamento de Astronomía y Astrofísica, Universidad de Concepcion, Chile

Abstract: A revised metallicity calibration of the Strömgren $(b-y), m_1$ diagram, based on a sample of globular cluster and field red giant stars, is presented. This new calibration has been used to determine Strömgren metallicities ($[\mathrm{Fe/H}]_{\mathrm{phot}}$) for more than 1400 red giants in ω Centauri. Most of the stars belong to a metal poor ($[\mathrm{Fe/H}]_{\mathrm{phot}} = -1.7$ dex), old population. A second more metal rich ($[\mathrm{Fe/H}]_{\mathrm{phot}} = -0.9$ dex) population is found to be about 3 Gyr younger and more centrally concentrated than the old one. The CN-rich stars do not seem to follow the radial distribution of the metal rich population.

1 Introduction

The globular cluster ω Centauri is known as an extraordinary object among the clusters of our Galaxy. It is not only the most massive and flattened Galactic globular cluster, but also shows strong variations in the abundances of CNO elements as well as in iron.

Whereas the CNO variations can be explained by evolutionary mixing effects in the stellar atmosphere as well as by primordial mixing, the iron abundance variations need another explication (e.g. Vanture et al. 1994, Norris & Da Costa 1995). Calcium abundance measurements of more than 500 red giants (Norris et al. 1996) show a bimodal metallicity distribution. About 80% of the stars have a low metallicity, the rest a 0.5 dex higher one. The interpretation is two succesive epochs of star formation after the self enrichment within the cluster over a relatively lengthy period. However, dynamical analysis of 400 stars in this sample (Norris et al. 1997) shows rotation in the metal poor component, whereas the metal rich one is not rotating. This favours a merger of two globular clusters with different masses, as shown by the model calulations of Makino et al. (1991).

Clearly, further analyses with large homogeneous samples are needed to understand the complex formation and enrichment history of this outstanding object.

*Based on data collected at the European Southern Observatory (La Silla, Chile)

1.1 Why Strömgren photometry?

Strömgren photometry has been proven to be a very useful metallicity indicator for globular cluster giants and subgiants (Richtler 1989, Grebel & Richtler 1992). The location of late type stars in the Strömgren $(b-y), m_1$ diagram is correlated with their metallicities, especially with their iron and CN abundances.

In the case of ω Centauri, CCD Strömgren photometry offers the possibility to determine metallicities and study iron and CNO abundances of a large number of stars simultaneously.

2 Observations and reduction

The observations have been performed in two observing runs in the nights 11-15 May 1993 and 21-24 April 1995 with the Danish 1.54m telescope at ESO/La Silla. The CCD in use was a Tektronix chip with 1024×1024 pixels. The $f/8.5$ beam of the telescope provides a scale of $15\farcs7$/mm, and with a pixel size of 24 μm the total field is $6\farcm3 \times 6\farcm3$. In total, 33 different fields have been observed in ω Cen (18 with short exposures, 15 with long exposures), 4 fields in M22 and 5 fields in M55. Figure 1 illustrates the selected fields in ω Cen.

The CCD frames were processed with the standard IRAF routines, instrumental magnitudes were derived using DAOPHOT II. After the photometric reduction, the matching of all frames, and calibration of the magnitudes, the average photometric errors for the red giants used for the metallicity determination are 0.011 mag for V, 0.016 mag for $(b-y)$ and 0.023 mag for m_1. More details are presented in Richter et al. (1999).

3 Revised metallicity calibration

Red giants in the globular clusters ω Cen, M55, and M22 together with field giants from Anthony-Twarog & Twarog (1998) have been used to revise the metallicity calibration of the Strömgren $(b-y), m_1$ diagram by Grebel & Richtler (1992). For all giants, accurate and homogeneous iron abundances from high resolution spectroscopy are available in the literature. In total, 58 CN-weak giants have been used. CN-rich stars have been excluded, since their m_1 value mimics a too high iron abundance in the $(b-y), m_1$ diagram. In order to cover a wide metallicity range, $-2.0 <$[Fe/H]< 0.0 dex, our new calibration is connected to a previous calibration by Grebel & Richtler (1992) around solar metallicities. In the color range $0.5 < (b-y) < 1.1$ mag, for which our calibration is valid, the loci of equal iron abundances lie on straight lines.

Following the calibration by Grebel & Richtler, a relation of the form

$$[\mathrm{Fe/H}] = (m_1 + a_1 \cdot (b-y) + a_2)/(a_3 \cdot (b-y) + a_4)$$

has been chosen for the fit. The derived coefficients are

$a_1 = -1.277 \pm 0.050$ $\quad$ $a_2 = \ \ 0.331 \pm 0.035$

$a_3 = \ \ 0.324 \pm 0.035$ $\quad$ $a_4 = -0.032 \pm 0.025$

The dispersion of the difference between the Strömgren metallicity and spectroscopic iron abundances is 0.11 dex, which indicates the average accuracy of the new calibration for a single giant. The detailed analysis of the metallicity calibration will be published in Hilker (1999).

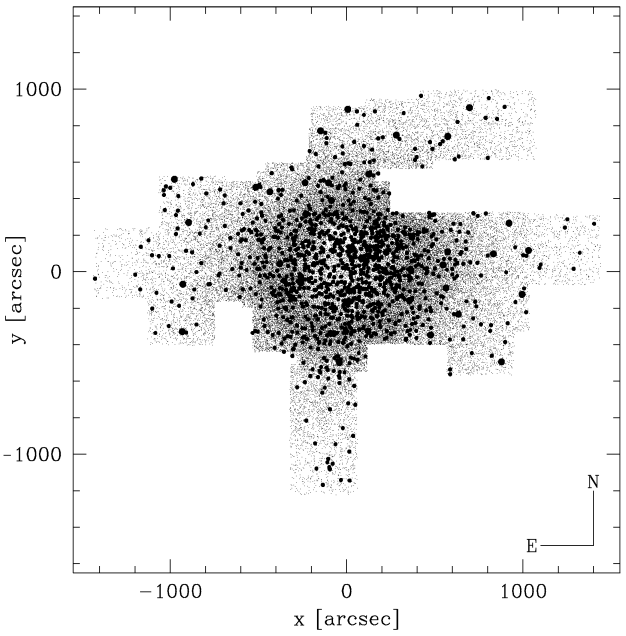

Figure 1: Position plot of all observed stars with a V magnitude brighter than 19.0 mag and a photometric error less than 0.1 mag. Bold dots indicate the position of selected red giants (see Fig. 2), large bold dots the ones with known spectroscopic abundances used in the metallicity calibration.

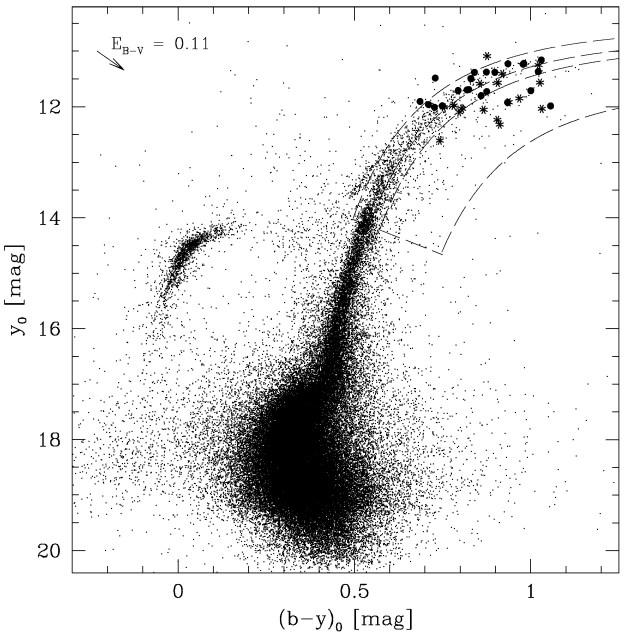

Figure 2: CMD of all stars with $\sigma_{rmphot} < 0.1$ mag. Filled circles indicate red giants with normal CN abundances, whereas stars marked with asterisks are known to be CN-strong. All stars within the area enclosed by dashed lines have been used for further analysis.

4 Analysis and Results

Figure 2 shows the color magnitude diagram of all observed stars in ω Cen with a photometric error less than 0.1 mag ($\simeq$ 92500 stars). The colors have been corrected for a reddening value of $E_{B-V} = 0.11$ mag (Zinn 1985). Bold dots and asterisks indicate the stars with known spectroscopic abundances which have been used for the metallicity calibration. The broad red giant branch at magnitudes brighter than $V = 14$ mag cannot be explained by photometric errors, but is due to a spread in age and metallicity. All stars in the CMD which are enclosed by the dashed lines were used for the metallicity determination ($\simeq$ 1400 stars). For further analysis the RGB was divided into three subsamples: a blue and a red side of the RGB, and all stars that are redder than the "main" RGB.

The metallicity spread is illustrated in the $(b-y), m_1$ diagram (Fig. 3) and the metallicity histogram (Fig. 4). Most of the blue RGB stars populate a prominent iso-metallicity line around -1.7 dex. These stars are not affected by CN enrichment and form a single metal poor population. Stars from the red side of the RGB have metallicities mainly in the range -1.3 to -0.5 dex. They appear well separated from the metal poor population. Stars with Strömgren metallicities higher than about -0.8 dex are supposed to be CN-rich stars of one of the two populations. However, lots of them are redder than the "main" RGB. Since their $(b-y)$ color is not influenced by CN variations, their existence in the CMD can only be explained by higher iron abundances. Therefore we conclude that there exists a true tail towards higher metallicities not only in the CN but also in the iron abundances.

Note that the numbers in the metallicity histogram do not represent the right proportion of metal poor to metal rich stars, since the stars have been selected due to a high accuracy in

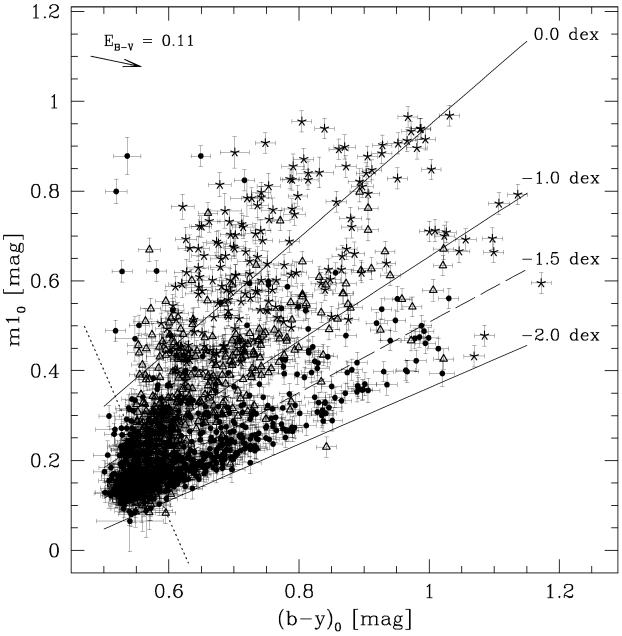

Figure 3: The $(b-y), m_1$ diagram for more than 1400 selected giants (see Fig. 2) is shown together with the lines of constant metallicity from the new calibration. The error bars include photometric and calibration errors. Dots indicate stars from the blue side of the RGB, triangles the ones from the red RGB side, and asterisks all stars lying apart from the "main RGB" (see Fig. 2).

Figure 4: In this plot the metallicity distribution of more than 1000 red giants and subsamples is shown. Only stars that are redder than the dotted line in Fig. 3 have been selected. The hashed histograms are the distributions of the "blue" RGB stars (metal poor), "red" RGB stars (more metal rich), and stars redder than the "main RGB", most of them being CN-rich.

metallicity (all stars redder than the dotted line in Fig. 3) and not due to a mass cut in the CMD. When accounting for a mass selected sample the ratio of metal poor to metal rich stars is about 3:1.

The different metallicities of the two populations have been used to estimate their ages. Since newly calculated isochrones in the Strömgren system still are missing, isochrones from Bergbusch & VandenBerg (1992), converted to Strömgren colors by Grebel & Roberts (1994), have been used. These isochrones were found to represent the shape of the RGB best, and therefore are very useful to determine relative ages. In Fig. 5 the two best fitting isochrones are shown. The metal poor stars ($-1.85 <$[Fe/H]< -1.55, bold dots) are best representated by an isochrone of 18 Gyr and -1.68 dex, the metal richer ones ($-1.2 <$[Fe/H]< -0.8, triangles) by an isochrone of 15 Gyr and -1.28 dex. The uncertainty in the age determination is about 1 Gyr. An isochrone of 18 Gyr for the red RGB stars cannot reproduce the narrow appearance of the CMD in the fainter RGB and turnover region. The fitted iron abundance is somewhat lower than the Strömgren metallicity of the metal rich population. This is due to the fact that CN-rich stars already influence the measurements in this metallicity range and pretend a too high metallicity.

The radial distribution of the different subpopulations in ω Cen is shown in Fig. 6. Only stars within a $6\farcm7$ wide strip west of the center of ω Cen have been selected, since these fields belong to the most homogeneous set of long exposures. The East-West axis is perpendicular to the rotation axis of the cluster. The metal richer and younger stars from the red side of the RGB are clearly more concentrated than the old metal poor population within 10 arcmin radius

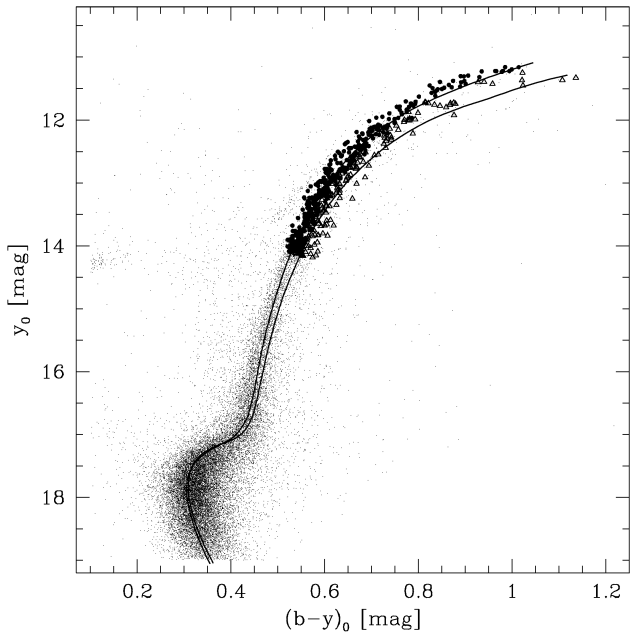

Figure 5: In this CMD isochrones from Bergbusch & VandenBerg (1992), converted to Strömgren colors by Grebel & Roberts (1994), have been fitted to the metal poor and more metal rich subpopulations in ω Cen. The corresponding ages and metallicities are indicated in the panel.

Figure 6: This plot shows the cumulative distribution of different subsamples of red giants in a 6.′7 wide strip west of the center of ω Cen. The selections are indicated in the panel. Clearly the metal richer stars are more concentrated than the old metal poor population.

from the cluster center. The situation is not that clear for the CN-rich stars. They seem to follow more the distribuion of the metal poor stars than that of the metal rich ones. However, this result has to be taken with caution, since number statistics are low, and this sample of stars most probably is a mix of CN enriched stars from both populations, and even foreground stars.

Putting all the facts from the metallicity determination, age estimation, and spatial distribution analyses together, there seems to be no doubt that ω Cen consists of (at least) two distinct populations of stars, which gives this extraordinary object more the characteristics of a galaxy than a globular cluster.

5 Summary

A new calibration of the Strömgren $(b-y), m_1$ diagram to the iron abundance of red giants has been presented. The Strömgren metallicity calibration is valid in the abundance range $-2.3 <$ [Fe/H] < 0.0 dex.

For Strömgren metallicities higher than -1.0 dex, CN-weak stars cannot be distinguished in the $(b-y), m_1$ diagram from stars with lower iron abundances but higher CN bands strength.

For more than 1400 red giants Strömgren metallicities have been determined. Besides a main metal poor ($[\mathrm{Fe/H}]_{rmphot} = -1.7$ dex) population, a more metal rich population ($[\mathrm{Fe/H}]_{rmphot} = -0.9$ dex), and a extended tail of CN-rich stars with higher Strömgren metallicities have been found.

The metal poor population is old. The metal richer population is about 3 Gyr younger and

more centrally concentrated than the old one.

Our findings are consistent with a scenario in which self enrichment within the cluster has been taken place over a period of about 2-4 Gyr with subsequent new star formation from the enriched and more concentrated material.

We point out that the conditions for such an enrichment history can be found in nuclei of dwarf galaxies, where the gas can be easily retained and a secondary star formation is common. The capture and dissolution of a nucleated dwarf galaxy by our Milky Way and the survival of ω Cen as its nuclues would be an attractive explanation for this extraordinary object.

Acknowledgements

We thank Boris Dirsch and Philipp Richter for helpful discussions and useful comments. This research was supported through 'Proyecto FONDECYT 3980032'.

References

Anthony-Twarog B.J., Twarog B.A., 1998, AJ 116, 1922
Bergbusch P.A., VandenBerg D.A., 1992, ApJS 81, 163
Grebel E.K., Richtler T., 1992, A&A 253, 359
Grebel E.K., Roberts W.J., 1995, AAS 186, 0308
Hilker M., 1999, A&A submitted
Makino J., Akiyama K., Sugimoto D., 1991, ApSS 185, 63
Norris J.E., Da Costa G.S., 1995, ApJ 447, 680
Norris J.E., Freeman K.C., Mayor M., Seitzer P., 1997, ApJ 487, L187
Norris J.E., Freeman K.C., Mighell K.J., 1996, ApJ 462, 241
Richter P., Hilker M., Richtler T., 1999, A&A in press
Richtler T., 1989, A&A 211, 199
Twarog B.J., Twarog B.A., 1998, AJ 116, 1922
Vanture A.D., Wallerstein G., Brown J.A., 1994, PASP 106, 835
Zinn R., 1985, ApJ 293, 424